Effects of Turbulence Manipulation in Skimming Flows: An Experimental Study

C.A. Gonzalez and H. Chanson

Department of Civil Engineering
The University of Queensland, Brisbane QLD, 4072 AUSTRALIA

Abstract

Current expertise in air-water flow properties in turbulent flows is limited to low to moderate Reynolds numbers and a few types of surfaces (roughness). Highly turbulent air-water flows cascading down a large-size stepped spillway model were systematically investigated with a 22° slope. Several stepped configurations were tested and turbulence manipulation was conducted to enhance interactions between skimming flows and cavity recirculating regions. Systematic experiments were performed with 3 new configurations to complement an initial study [6] with another three configurations. Turbulence modifiers (vanes or longitudinal ribs) were observed to have a strong influence on the air-water flow properties, with wakes or low-speed streaks observed above each vane.

Introduction

Numerous studies of turbulent flows over rough surfaces were conducted with different approaches [1,10,14]. However, only a limited number of the published papers refer to highly turbulent flows associated with strong free-surface aeration [3,7]. One such flow situation is a high velocity open channel flow skimming down a stepped canal (Figure 1). This type of channel design is common for overflow spillways of gravity and embankment dams [4]. Most structures were designed with flat horizontal steps but some included devices to enhance energy dissipation [6]. There may be some analogy between skimming flows over stepped chutes and skimming flows above large roughness elements, including boundary layer flows past d-type roughness. Chanson and Toombes [7] presented new experimental evidence for the former. Djenidi et al [10] provided a comprehensive review of the latter configuration, while Aivazian [1] studied zigzag strip roughness. Mochizuki et al [13,14] studied turbulent boundary layer past d-type roughness with thin longitudinal ribs. Despite conflicting interpretations of their data, their experiments demonstrated some turbulence manipulation by interfering with the recirculation vortices.

Chanson and Gonzalez [6] demonstrated a strong influence of the vanes on the air-water flow properties of both free-stream and cavity recirculation flows, as the vanes prevented the spanwise translation of cavity recirculating eddies and contributed to the development of low speed streaks above each vane. They also suggested that the microscopic air-water flow structure (bubble/droplet distribution and clustering) was affected by the presence of vanes possibly leading to form drag and energy dissipation enhancement. Their results hinted that more intricate vane arrangements could disturb further the flow.

This paper presents the result of an investigation into the effects at microscopic scales of several vane configurations. The experiments were conducted in a large stepped channel equipped with 3 new vane arrangements operating with Reynolds numbers between 4 and 9 E+5 (Figure 1, table 1). Interactions between free surface and cavity recirculation, as well as turbulence manipulation were systematically investigated in skimming flow regime.

Experimental Facilities

New experiments were conducted at the University of Queensland in a 3.3 m long, 1 m wide, 21.8° slope chute for flow rates ranging from 0.10 to 0.22 m³/s corresponding to a skimming flow regime with Reynolds numbers between 4 and 9 E+5 (table 1).

The water supply pump was controlled by an adjustable frequency AC motor drive. This enabled for the accurate control of the closed circuit system. Waters were supplied from a feeding basin (1.5 m deep, surface area 6.8 m × 4.8 m) leading to a sidewall convergent with a 4.8:1 contraction ratio. The test section was a broad-crested weir (1 m wide, 0.6 m long, with upstream rounded corner (0.057 m radius) followed by ten identical steps (h = 0.1 m, l = 0.25 m) made of marine ply (Figure 1). The stepped chute was 1 m wide with perspex sidewalls followed by a horizontal concrete-invert canal ending in a dissipation pit. For three series of experiments, vanes (longitudinal thin ribs) were placed among the step cavities in different configurations to modify turbulence and possibly to enhance energy dissipation (Figure 2, table 1).

Figure 1. Skimming flow down a stepped chute (h = 0.1 m) (Configuration 3 d_c/h = 1.3, Re = 7.3 E+5). Left: side view. Right: Top view with flow from top to bottom.
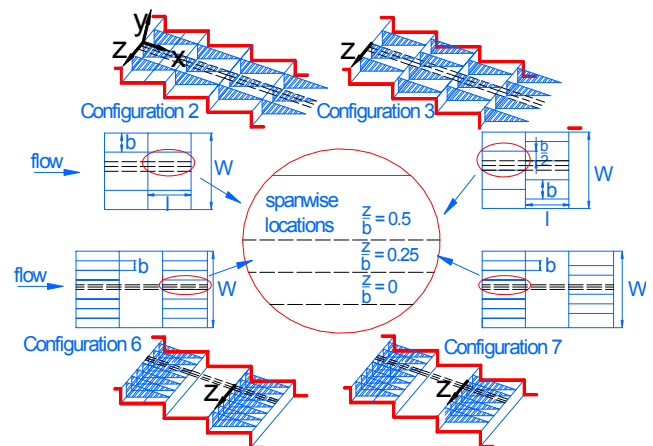

Figure 2. Sketch of a stepped invert with energy dissipation enhancers.

Clear-water flow depths were measured with a point gauge and air-water flow properties with a double-tip conductivity probe (∅ = 0.025 mm) designed at the University of Queensland [2] (Figure 3). The probe sensors were aligned in the free-stream flow direction. The leading tip had a small frontal area (i.e. 0.05 mm²) and the trailing tip was offset to avoid wake disturbance from the first tip. Tests showed the absence of wake disturbance during all experiments [2].

An air bubble detector (UQ82.518) excited the probe and its output signal was scanned at 20 kHz for 20 s. The translation of the probes in the direction normal to the channel invert was controlled by a fine adjustment travelling mechanism connected to a Mitutoyo™ digimatic scale unit. The error on the vertical position of the probe was less than 0.025 mm. The accuracy on the longitudinal probe position was estimated as $\Delta x < +/- 0.5$ cm. The accuracy on the transverse position of the probe was less than 1mm. Flow visualizations were conducted with high-shutter speed digital still and video cameras.
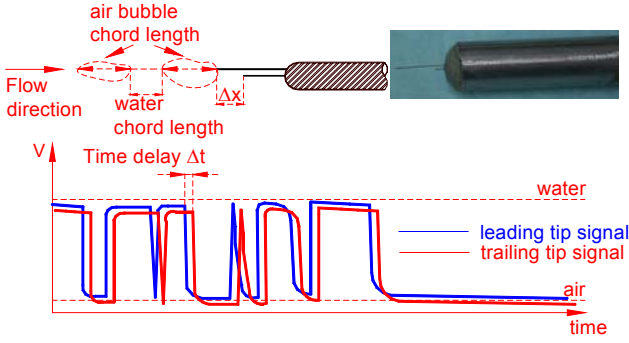

Figure 3. Sketch and photo of the double-tip conductivity probe and corresponding binary signal.

Measurements were performed at step edges and between adjacent step edges within the main flow stream and into the recirculation cavity region observed below the pseudo-bottom formed by the step edges. For the stepped configurations with vanes, measurements were conducted at spanwise locations z/b = 0, 0.25 & 0.5, where z is the spanwise direction with z = 0 at the centre of the channel above an arrangement of vanes and b is the spacing between vanes (Figure 2).

Reference	θ^o	q_w (m²/s)	h (m)	Re	Remarks
(1)	(2)	(3)	(4)	(5)	(6)
Chanson & Gonzalez [6]	21.8	0.1 to 0.22	0.1	4E+5 to 8.7E+5	L=3.3 m, W=1m
Config. 1	b=W=1m (no vane)				
Config. 2	b = W/4 = 0.25 m (3 vanes in line)[6]				
Config. 4	b = W/8 = 0.125 m (7 vanes in line)[6]				
Config. 5	b = W/8 = 0.125 m (7 vanes in zigzag)[6]				
Present Study	21.8	0.1 to 0.22	0.1	4E+5 to 8.7E+5	L=3.3 m, W=1 m
Config. 3	b=W/4=0.25m(3 vanes in zigzag every step)				
Config. 6	b=W/8=0.125m(7 vanes in line every 2 steps)				
Config. 7	b=W/8=0.125m(7 vanes in zigzag every 2 steps)				
Notes: h : step height; W chute width; L : chute length					

Table 1. Detailed experimental investigations on moderate slope stepped chutes with turbulence manipulation.

Data Analysis

The probe sampled data that provided information about the void fraction, bubble count rate, velocity, turbulence intensity, and air/water chord length distributions [5,10]. The void fraction or air concentration C is the proportion of time that the probe tip is in the air. The bubble count rate F is the number of bubbles impacting the probe tip. The bubble chord length provides information on the air-water flow structure. With a double-tip conductivity probe, the velocity measurement is based upon the successive detection of air-water interfaces by both tips.

In turbulent air-water flows, the detection of all bubbles by each tip is highly improbable and it is common to use a cross-correlation technique [9]. The time average air-water velocity equals:

$$V = \frac{\Delta x}{T} \qquad (1)$$

where Δx is the distance between tips and T is the time for which the cross-correlation function is maximum. The turbulent intensity may be derived from the broadening of the cross-correlation function compared to the autocorrelation function:

$$Tu = 0.851 \cdot \frac{\sqrt{\Delta T^2 - \Delta t^2}}{T} \qquad (2)$$

where T is a time scale satisfying : $R_{xy}(T+\Delta T) = 0.5*R_{xy}(T)$, R_{xy} is the normalized cross correlation function, and t the characteristic time for which the normalized autocorrelation function R_{xx} equals 0.5 [5]. Thin skewed cross-correlation functions correspond to small variation in the interfacial velocity, hence small turbulent levels. Broad cross-correlation functions imply large turbulence levels.

Chord sizes may be calculated from the raw probe signal outputs. The results provide a complete characterization of the stream wise distribution of air and water chords. In turn information on the flow structure may be analyzed in terms of particle clustering and grouping [7]. In this study, two air bubbles are considered to be part of a cluster when the water chord separating the bubbles is less than one tenth of the mean water chord size. The measurement of air-water interface area is a function of void fraction, velocity, and bubble sizes. For any bubble shape, bubble size distribution and chord length distribution, the specific air-water interface area a defined as the air-water interface area per unit volume of air and water may be derived from continuity:

$$a = 4 \cdot \frac{F}{V} \qquad (3)$$

where F is the bubble count rate and V the velocity.

Flow Observations

Skimming flows look similar to self-aerated flows down smooth chutes (Figure 1). At the upstream end, the flow was smooth and transparent. However, a bottom boundary layer developed. When the outer edge of the boundary layer reached the water free surface, turbulence induced strong aeration. Downstream of the point of inception of air entrainment, air-water flow became fully developed and "white waters" were observed. Strong exchanges of air-water and momentum occurred between the main stream and the atmosphere. Intense cavity recirculation was observed also below the pseudo-invert formed by the step edges. The air-water flow mixture consisted of a bubbly region(C < 30%), a spray region (C > 70%) and an intermediate zone in between.

Observations from the sidewall showed some effects of the vanes on cavity recirculation. Vanes appeared to be subjected to strong pressure and shear forces. Fluctuations seemed to be of the same period and in phase with cavity fluid ejections reported by Djenidi et al. [10] for d-type roughness and Chanson et al. [8] for stepped chute flows. Longitudinal troughs above the vanes were also observed possibly associated with wakes or quasi-coherent low speed streaks occurring immediately above each vane.

Air-Water Flow Properties

A detailed comparison of measured air-water flow properties obtained at z/b = 0, 0.25 and 0.5 for stepped configurations with vanes was conducted and compared with data for a stepped geometry without vanes. Figure 4 presents typical results of air concentration C and velocity V/V_{90} for configurations 6 & 7 at step edge 9, where y is the distance normal to the pseudo-bottom formed by the step edges, Y_{90} the distance where C = 0.90 and V_{90} is the air-water flow velocity at $y =Y_{90}$.

Void fraction distributions observed in Figure 4 suggested negligible effects of the vanes on the rate of air entrainment. Velocity measurements at all transverse positions for each vane

configuration showed some marked difference in presence of vanes within $y/Y_{90} < 0.6$ to 0.7 demonstrating that the effect of the vanes was not limited to the cavity flow but extended into the mainstream, result that is consistent with a wake region observed nearby the wall of each vane.

Figure 5 presents velocity V/V_{90} and turbulence intensity Tu distributions obtained for configurations 1 & 7 (7 vanes in zigzag every 2 steps) between step edges 9 and 10 (step cavity without vanes). Results hinted that the streamwise effects of vanes are limited to one downstream cavity as hardly any difference in velocity and turbulence intensity could be observed despite the presence of vanes.
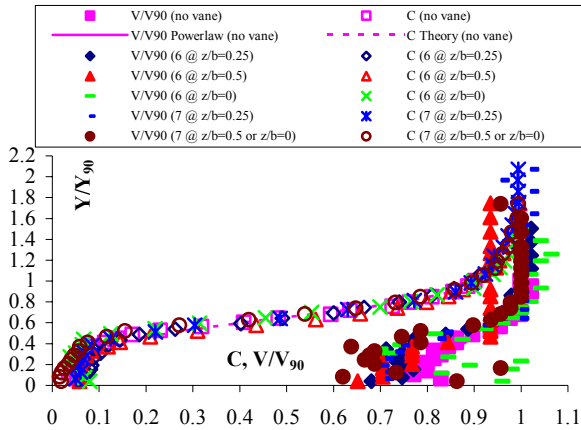

Figure 4. Void fraction and velocity distributions at step edge 9 (dc/h=1.5). Comparison between Configuration 1 (No vane) and every configuration including 7 vanes (Config. 4,5,6,7).
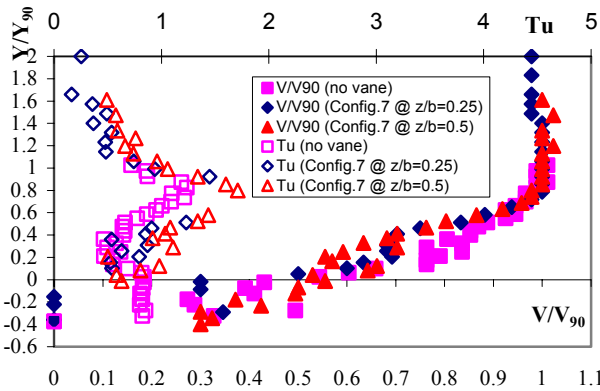

Figure 5. Turbulence intensity and velocity distributions at one quarter of the distance between step edges 9 and 10 ($d_c/h = 1.5$). Comparison between Configuration 1 (No vane) and configuration 7 (7 vanes in zigzag every 2 steps).

Flow Resistance and Energy Dissipation

Flow resistance was calculated from the average friction slope [8] for all the configurations at z/b=0(above vanes), 0.25 and 0.5 (table 2). Results are presented in Table 2 for all configurations. In average they implied equivalent Darcy friction factors of 0.16, 0.21, 0.21 and 0.20 in average for no vane, 3 and 7 vanes inline and 7 vanes in line every 2 steps respectively and 0.22, 0.22 and 0.21 in average for 3 and 7 vanes in zigzag and 7 vanes in zigzag every 2 steps respectively suggesting that the presence of vanes increased the flow resistance and the rate of energy dissipation. Maximum values of equivalent Darcy friction f_e factors were observed for configurations with vanes in zigzag (Configurations 3, 5 & 7). However, results of f_e obtained for configuration 7 were smaller than those corresponding to configuration 5.

Air-Water Chord length Distributions

In highly turbulent air-water flow, measurements with intrusive phase-detection probe, were analysed in terms of streamwise air or water structures bounded by air-water interfaces detected by the probe tip (Figure 3). Figure 6 presents probability distribution functions (PDF) of bubble chord sizes corresponding to configurations 1, 2 and 3 obtained below the pseudo-bottom formed by the step edges (y/h < 0). Figure 7 presents PDF of bubble chords for the same configurations in locations above the pseudo-bottom (y/h > 0) with similar void fractions. Results showed a greater number of bubbles detected in the mainstream (y/h > 0) and a broader range of bubble sizes at locations below the pseudo-bottom, in agreement with previous observations [7]. Note the differences between Figures 6 and 7, where the amount of bubbles detected in the mainstream (Fig. 7) were at least twice as much as that detected in the recirculation region (Fig. 6), for locations with very similar void fraction. The histogram mode (predominant bubble size) was between 0.5 and 1 mm for all configurations at both locations (y/h < 0 & y/h > 0) suggesting that the flow structure did not vary much for configurations 1, 2 & 3 (No vane, 3 vanes in line and 3 vanes in zigzag respectively).

Conf.	f_e					
	1	2			3	
	No vane	3 vanes in line			3vanes in zigzag	
d_c/h		z/b=0	z/b=0.25	z/b=0.5	z/b=0.25	z/b=0.5
1.1	0.1689	0.2384	0.1673	0.1863	0.1412	0.2118
1.3	0.1756	0.236	0.1859	0.1728	0.1506	0.2867
1.5	0.0924	0.3109	0.1446	0.1334	0.2075	0.2882
1.7	0.211	0.2713	0.1911	0.2585	0.2253	0.227
Conf	4			5		
	7 vanes in line			7 vanes in zigzag		
d_c/h	z/b=0	z/b=0.25	z/b=0.5	z/b=0.25	z/b=0&0.5	
1.1	-	0.1741	0.1704	0.1796	0.2377	
1.3	-	0.1699	0.1755	0.2051	0.3112	
1.5	0.2806	0.1649	0.1656	0.2105	0.2487	
1.7	-	0.1704	0.1628	0.2152	0.1696	
Conf	6			7		
	7 vanes in line every 2 steps			7 vanes in zigzag every 2 steps		
d_c/h	z/b=0	z/b=0.25	z/b=0.5	z/b=0.25	z/b=0&0.5	
1.1	0.2155	0.177	0.1807	0.1649	0.2047	
1.3	0.2579	0.167	0.191	0.1196	0.2364	
1.5	0.2659	0.1626	0.16	0.136	0.2306	
1.7	0.3735	0.1208	0.1626	0.207	0.3464	

Notes: d_c: critical depth

Table 2. Flow resistance estimates in air-water flows
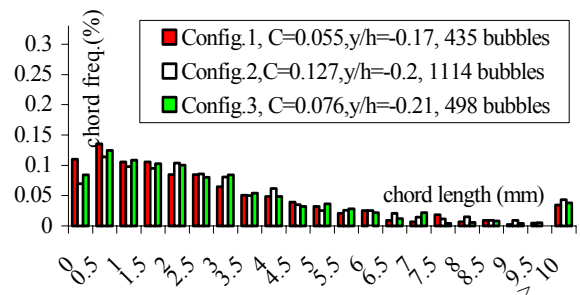

Figure 6. Air-bubble chord length PDF. dc/h=1.5 between step edges 9 and 10 at X=0.25 and z/b=0.25 (y/h < 0).
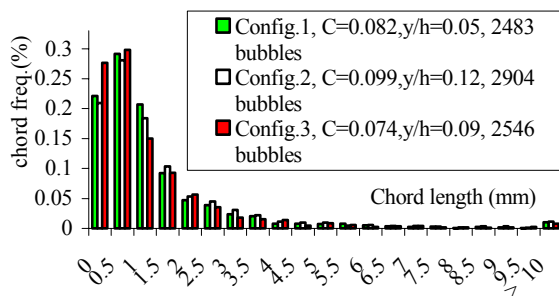
Figure 7. Air-bubble chord length PDF. dc/h=1.5 between step edges 9 and 10 at X=0.25 and z/b=0.25 above pseudo-bottom (y/h > 0).

Bubble Clustering

For configurations 1 and 3, air-bubble and water-droplet clustering analyses were performed at several flow positions (e.g. from bubbly to spray region) and at different streamwise locations along the cavity (X = 0.25, 0.5 & 0.75). Results demonstrated consistency with previous studies [7,8] confirming that a great proportion of bubbles (typically 30%) clustered mainly in 2 particles. Despite recirculating eddy presence and mixing layer influence the flow structure did not vary much.

Discussion

Holmes et al [12] proposed the existence of pairs of counter-rotating streamwise eddies next to the wall in turbulent boundary layers, associated with a region of reduced velocity in the stream direction. Above vanes, quasi-coherent wakes, somehow similar to low-speed streaks, were seen interfering with the main stream.

It is believed that the effects of the vanes onto the main flow were two-fold. Firstly the presence of vanes prevented the spanwise development of large coherent structures in the step cavities (y/h < 0). Secondly they led to the appearance of longitudinal (streamwise) coherent "wake" structures in the mainstream flow (y/h > 0). Such coherent structures affects momentum exchange between cavity and stream flows, enhancing vertical mixing between recirculation zones and mainstream and hence the rate of energy dissipation. Such vertical mixing is characterized by irregular fluid ejections, turbulent bursts and sweeps.

In terms of flow resistance maximum equivalent Darcy friction factors f_e were found for configurations with vanes in zigzag (Configurations 3, 5 & 7). However, results obtained for configuration 7 were smaller than those corresponding to configuration 5. Based upon such finding, it is hypothesized that the behaviour of recirculating vortices is different for every vane arrangement. It is believed that, for configuration 7, the spanwise development of the recirculating eddies in the step cavities reappeared where no vanes existed (every 2 steps) inducing smaller flow resistance than configurations where the vortices remained confined in small cavities at all times (with vanes at each step).

Conclusion

Interactions between free surface and cavity recirculation, as well as turbulence manipulation were investigated in skimming flow regime down a stepped chute in a large facility operating with highly turbulent flows. Three new turbulence manipulation arrangements were tested and compared with previous data [6]. Results demonstrated that the vane arrangements influence in a different manner the air-water flow properties in both mainstream and recirculating region. Maximum flow resistance was observed for configurations with vanes arranged in zigzag while flow resistance for configuration 7 (zigzagged vanes placed every 2 steps) was smaller than that corresponding to configuration 5 (zigzagged vanes placed every step).

Based upon presented results it is hypothesized that maximum flow resistance and greatest interfacial aeration are achieved with zigzagged geometries placed at each step, rather than inline vane arrangements. It is also suggested that more intricate geometries (e.g. zigzagged vanes every 2 steps) will not further flow resistance. This study provides new information on the complex structure of highly turbulent aerated flows and suggests that turbulence manipulation can be applied to stepped spillways to enhance energy dissipation and to aeration cascades to enhance re-oxygenation.

References
[1] Aivazian, O.M., New Investigations and new Method of Hydraulic Calculation of Chutes with Intensified Roughness.*Gidrotekhnicheskoe Stroitel'stvo*, No. **6**, 1996, 27-39 (in Russian).

[2] Chanson, H., Air Bubble Entrainment in Free-surface Turbulent Flows. Experimental Investigations. *Report CH46/95*, Dept. of Civil Engineering, University of Queensland, Australia, 1995.

[3] Chanson, H., *Air Bubble Entrainment in Free-Surface Turbulent Shear Flows*. Academic Press, 1997.

[4] Chanson, H., *The Hydraulics of Stepped Chutes and Spillways*. Balkema, 2001.

[5] Chanson, H.. Air-Water Flow Measurements with Intrusive Phase-Detection Probes. Can we Improve their Interpretation ?. *Jl of Hyd. Engrg.*, ASCE, Vol. **128**, No. **3**, 2002 , 252-255.

[6] Chanson, H., and Gonzalez, C.A., Interactions between Free-surface, Free-stream Turbulence and Cavity Recirculation in Open Channel Flows: *Measurements and Turbulence Manipulation. 5th International Conference on Multiphase Flow, ICMF'04, Yokohama, Japan*, 2004 Paper No. **104**.

[7] Chanson, H., and Toombes, L., Air-Water Flows down Stepped Chutes: Turbulence and Flow Structure Observations. *Intl Jl of Multiphase Flow*, Vol. **27**, No. **11**, 2002, 1737-1761.

[8] Chanson, H., Yasuda, Y., and Ohtsu, I., Flow Resistance in Skimming Flows and its Modelling. *Can. Jl. of Civ. Eng.*, Vol. **29**, No. **6**, 2002, 809-819.

[9] Crowe, C., Sommerfield, M., and Tsuji, Y., *Multiphase Flows with Droplets and Particles*. CRC Press, 1998.

[10] Djenidi, L., Elavarasan, R., and Antonia, R.A., The Turbulent Boundary Layer over Transverse Square Cavities. *Jl Fluid Mech.*, Vol. **395**, 1999, 271-294.

[11] Gonzalez, C.A., and Chanson, H., Interactions between Cavity Flow and Main Stream Skimming Flows: an Experimental Study. *Can Jl of Civ. Eng.*, Vol. **31**,2004.

[12] Holmes, P., Lumley, J.L., and Berkooz, G., Turbulence, *Coherent Structures, Dynamical Systems and Symmetry*.Cambridge University Press, 1996. pp. 63-77.

[13] Mochizuki, S., and Osaka, H., Two-Point Velocity Correlation Measurement in a d-type Rough Wall Boundary Layer Modified with the Longitudinal Thin Ribs: *Proc. 9th Symp. On Turbulent Shear Flows*, Kyoto, Japan, (1993), paper 5-2.

[14] Mochizuki, S., Izawa, A., and Osaka, H., "Turbulent Drag Reduction in a d-type Rough Wall Boundary Layer with Longitudinal Thin Ribs Placed within Traverse Grooves Higher-order Moments and Conditional Sampling Analysis)." *Trans. JSME Intl Journal*, series B, Vol. **39**, No. **3**, 1996, 461-469.